

Modeling of Massive Inductors with the H - Φ Magnetodynamic Formulations via a Finite Element Technique

Vuong Dang Quoc

Hanoi University of Science and Technology - No. 1, Dai Co Viet, Hai Ba Trung, Hanoi, Viet Nam

Received: May 25, 2020; Accepted: June 22, 2020

Abstract

Magnetodynamic problems are present everywhere in electrical systems in general and electrical equipments in particular. Thus, studying magnetodynamic problems becomes very important in the electromagnetic devices and is always topical subjects for researchers and designers in worldwide. The idea of this paper is to compute and simulate the distribution of local and global fields (magnetic flux density, magnetic field, eddy current, joule loss, current and voltage) in conducting and non-conducting regions. The H - Φ magnetodynamic formulations is proposed for massive inductors in order to link/couple with circuit equations defining currents or voltages. The method allows to solve problems in high frequency domains to take skin depths and skin effects into account.

Keywords: Current, voltage, joule power loss, eddy current, magnetic field, skin effect, numerical method

1. Introduction

Modeling of electromagnetic problems plays an essential role in electrical systems in general and electrical equipments in particular. Many papers have been recently applied many different methods (e.g. the finite element method, finite differential method and boundary method) for dealing with magnetodynamic problems with low frequencies which current densities are fixed in stranded inductors [4-7]. This means that skin effects with high frequencies do not take into account.

In this challenge, a finite element technique with the h - Φ magnetodynamic formulations is presented for massive inductors coupled to circuit equations where either voltages or currents can be fixed to compute local and global fields (magnetic field distributions, electric fields, eddy current losses, joule power losses, electromotive forces and skin effects) with high frequencies [1, 2]. The validation of the method is applied to a practical test [9].

2. Definition of magnetodynamic problems

A magnetodynamic problem is presented in a studied domain Ω , defining boundary conditions (BCs) $\partial\Omega = \Gamma = \Gamma_h \cup \Gamma_e$ in a space of Eculidean \mathfrak{R}^3 . The set of Maxwell's equations and constitutive behaviors can be written as [1]-[8]:

$$\text{curl } \mathbf{E} = -\partial_t \mathbf{B}, \text{ curl } \mathbf{H} = \mathbf{J}_s, \text{ div } \mathbf{B} = 0, \quad (1a-b-c)$$

where constitutive behaviors give:

$$\mathbf{B} = \mu \mathbf{H}, \mathbf{J} = \sigma \mathbf{E}, \quad (2a-b)$$

with BCs:

$$\mathbf{n} \times \mathbf{E}|_{\Gamma_e} = 0, \quad (3)$$

where \mathbf{B} [T] is the magnetic induction, \mathbf{H} (A/m) is magnetic field, \mathbf{E} (V/m) is the electric field, \mathbf{J} (A/m²) is the eddy current, μ and σ are the magnetic permeability and electric conductivity, respectively. \mathbf{J}_s (A/m²) is the imposed electric current presented in non-conducting regions Ω_c^c , with $\Omega_c = \Omega_c \cup \Omega_c^c$ and \mathbf{n} is the unit normal vector.

Maxwell's equations are solved with the associated BC given in (3) taken the tangential component into account.

For magnetodynamic cases, the fields $\mathbf{H}, \mathbf{B}, \mathbf{E}, \mathbf{J}$ are checked to satisfy the Tonti diagram [3]. This means that the fields $\mathbf{H} \in \mathbf{H}_h(\text{curl}; \Omega)$, $\mathbf{J} \in \mathbf{H}_h(\text{div}; \Omega)$, $\mathbf{E} \in \mathbf{H}_e(\text{curl}; \Omega)$ and $\mathbf{B} \in \mathbf{H}_e(\text{div}; \Omega)$, where function spaces $\mathbf{H}_h(\text{curl}; \Omega)$ and $\mathbf{H}_e(\text{div}; \Omega)$ present existed fields on boundaries Γ_h and Γ_e of Ω . Hence, Tonti's diagram of the magnetodynamic problem is expressed as [3, 10]:

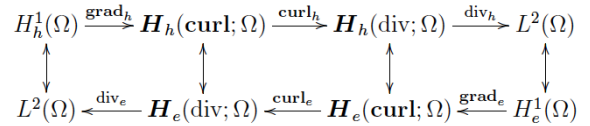


Fig. 1. Tonti's diagram [10].

3. Discretization with magnetic field formulations

Discretized equations with magnetic field formulations are established due to the set of

* Corresponding author: Tel.: (+84) 963286734
Email: vuong.dangquoc@hust.edu.vn

Maxwell's equations (1a-b-c) and the behavior laws (2a-b). In general, to satisfy the Ampere law (1 b), the fields $\mathbf{H} \in \mathbf{H}_h(\text{curl}; \Omega)$, $\mathbf{J} \in \mathbf{H}_h(\text{div}; \Omega)$, $\mathbf{E} \in \mathbf{H}_e(\text{curl}; \Omega)$ and $\mathbf{B} \in \mathbf{H}_e(\text{div}; \Omega)$ must be verified and satisfied the constitutive laws presented in (2a-b). Thus, based on the Faraday law, the discretized equation is written as [5, 7]:

$$\int_{\Omega} \partial_t(\mathbf{B} \cdot \mathbf{H}') d\Omega + \int_{\Omega} \text{curl} \mathbf{E} \cdot \mathbf{H}' d\Omega = 0, \\ \forall \mathbf{H}' \in \mathbf{H}_h^0(\text{curl}; \Omega), (4)$$

where $\mathbf{H}' \in \mathbf{H}_h^0(\text{curl}; \Omega)$ is a test function does not depend on time. By applying a Green formulation to (4), one has:

$$\int_{\Omega} \partial_t(\mathbf{B} \cdot \mathbf{H}') d\Omega + \int_{\Omega} \text{curl} \mathbf{E} \cdot \mathbf{H}' d\Omega \\ + \int_{\Gamma} (\mathbf{n} \times \mathbf{E}) \cdot \mathbf{H}' d\Gamma = 0, \\ \forall \mathbf{H}' \in \mathbf{H}_h^0(\text{curl}; \Omega). (5)$$

Combination (5) with behavior laws in (2 a-b), it is rewritten as:

$$\int_{\Omega} \partial_t(\mu \mathbf{H} \cdot \mathbf{H}') d\Omega + \int_{\Omega} \sigma^{-1} \text{curl} \mathbf{H} \cdot \text{curl} \mathbf{H}' d\Omega \\ + \int_{\Omega} \mathbf{e} \cdot \text{curl} \mathbf{H}' d\Omega \\ + \int_{\Gamma} (\mathbf{n} \times \mathbf{E}) \cdot \mathbf{H}' d\Gamma = 0. \\ \forall \mathbf{h}' \in \mathbf{H}_h^0(\text{curl}; \Omega). (6)$$

The field \mathbf{H} in (6) is decomposed into two parts [10]:

$$\mathbf{H} = \mathbf{H}_r + \mathbf{H}_s, (7)$$

where, \mathbf{H}_s is a source field defined via an imposed electric current in massive inductors and \mathbf{H}_r is a reaction field what needs to be defined through

$$\begin{cases} \text{curl} \mathbf{H}_s = \mathbf{j}_s & \text{in } \Omega_{ms} \\ \text{curl} \mathbf{H} = 0 & \text{in } \Omega_c^c - \Omega_{ms} \end{cases} (8)$$

for

$$\text{curl} \mathbf{H} = \mathbf{0} \text{ in } \Omega_c^c. (9)$$

It should be noted that in the non-conducting regions Ω_c^c , the field \mathbf{H}_r can be defined via a magnetic scalar potential ϕ such that $\mathbf{h}_r = -\text{grad} \phi$. The scalar potential ϕ in Ω_c^c is the multi-value made a single-value through cuts in the hole of Ω_c [7].

The field \mathbf{H}' in the discretized equation (6) is defined as a sub-space of $\mathbf{H}_h^0(\text{curl}; \Omega)$, for $\text{curl} \mathbf{H}' = \mathbf{0}$ in Ω_c^c , and $\mathbf{H}' = \mathbf{H}'_r + \mathbf{H}'_s$. The third integral in (6) is equal to zero in Ω_c^c . Therefore, combination of (6) and (7), one has:

$$\int_{\Omega} \partial_t(\mu \mathbf{H}_r \cdot \mathbf{H}') d\Omega + \int_{\Omega} \partial_t(\mu \mathbf{H}_s \cdot \mathbf{H}') d\Omega \\ + \int_{\Omega} \sigma^{-1} \text{curl} \mathbf{H}_r \cdot \text{curl} \mathbf{H}' d\Omega \\ + \int_{\Gamma} (\mathbf{n} \times \mathbf{E}) \cdot \mathbf{H}' d\Gamma = 0, \\ \forall \mathbf{H}' \in \mathbf{H}_h^0(\text{curl}; \Omega),$$

with $\text{curl} \mathbf{H}'_r = \mathbf{0}$ in Ω_c^c and $\mathbf{H}' = \mathbf{H}'_r + \mathbf{H}'_s$, (10)

where $\mathbf{H}_h^0(\text{curl}; \Omega)$ is defined in Ω and contains the basis function and test function of \mathbf{H} linked to the scalar potential ϕ .

The tangential component $(\mathbf{n} \times \mathbf{E})$ in the discretized equations of (10) is presented on the boundary Γ_e of Ω and is considered as a natural BC given in (3). If nonzero, it is defined as massive inductors presented in Section 2.2.

3.1. Global quantities in massive inductors

In (10), the electric field $\mathbf{E} = \mathbf{E}_s$ in massive inductors Ω_{ms} is unknown and its circulation is defined via one electrode of Ω_{ms} imposed by the applied voltage V_i [10]. Moreover, the surface integral in (10) can be expressed, i.e. $\mathbf{H}' = \mathbf{c}_i$ [10], for the boundary of the massive inductor Ω_{ms} :

$$\int_{\Gamma} (\mathbf{n} \times \mathbf{E}) \cdot \mathbf{H}' d\Gamma = \int_{\Gamma} (\mathbf{n} \times \mathbf{E}_s) \cdot \mathbf{c}_i d\Gamma = \\ - \int_{\Gamma} (\mathbf{n} \times \mathbf{E}_s) \cdot \text{grad} q_i d\Gamma \\ = \int_{\Gamma} (\text{grad} q_i \times \mathbf{E}_s) \cdot \mathbf{n} d\Gamma \\ = \int_{\Gamma} \text{curl}(q_i \mathbf{E}_s) \cdot \mathbf{n} d\Gamma \\ - \int_{\Gamma} q_i \text{curl} \mathbf{E}_s \cdot \mathbf{n} d\Gamma. (11)$$

By using the Stokes formula, the second integral on RHS of (11) is

$$\int_{\Gamma} (\mathbf{n} \times \mathbf{E}_s) \cdot \mathbf{c}_i d\Gamma = \oint_{\partial\Gamma} q_i \mathbf{E}_s \cdot d\mathbf{l} = \oint_{\gamma} \mathbf{E}_s \cdot d\mathbf{l} \\ = V_i (12)$$

where γ is the part of the oriented contour $\partial\Gamma$. In the same way, the test function $\mathbf{H}' = \mathbf{c}_i$ with (12), equation (10) becomes

$$\int_{\Omega} \partial_t(\mu \mathbf{H}_r \cdot \mathbf{c}_i) d\Omega + \int_{\Omega} \sigma^{-1} \text{curl} \mathbf{H}_r \cdot \mathbf{c}_i d\Omega = -V_i, \\ \forall \mathbf{c}_i \in \mathbf{H}_h^0(\text{curl}; \Omega). (13)$$

The equation (10) is a circuit equation for massive inductors.

3.2. Discretization of fields H_r and Φ

In (13), the field H_r is discretized with edge finite elements with the function space $H_h^0(\text{curl}; \Omega)$ expressed in the mesh of Ω , that is [10]

$$H_r = \sum_{e \in E(\Omega)} H_e s_e, \quad (14)$$

where $E(\Omega)$ is the set of edges of Ω , s_e is a shape function associated with the edge “ e ”, and H_e is the circulation of H_r along the edge “ e ”. In this study, the mesh elements are triangle and rectangular elements. As presented, the field $H_r = 0$ in Ω_c^c , thus $H_r = -\text{grad } \phi$. Hence, the scalar potential is expressed as [4]:

$$\phi = \sum_{n \in N(\Omega_c^c)} \phi_{c,n} v_{c,n} \quad (15)$$

where the field $\phi_{c,n}$ is defined in the non-conducting region. The discretization of $H_r - \phi$ is rewritten as:

$$H_r = \sum_{e \in E(\Omega_c)} H_e s_e + \sum_{n \in N(\Omega_c^c)} \phi_{c,n} v_{c,n}. \quad (16)$$

Now, by substituting (16) into (13), one gets:

$$\int_{\Omega} \partial_t \sum_{e \in E(\Omega_c)} H_e s_e \cdot c_i d\Omega + \int_{\Omega} \partial_t \sum_{n \in N(\Omega_c^c)} \phi_{c,n} v_{c,n} \cdot c_i d\Omega$$

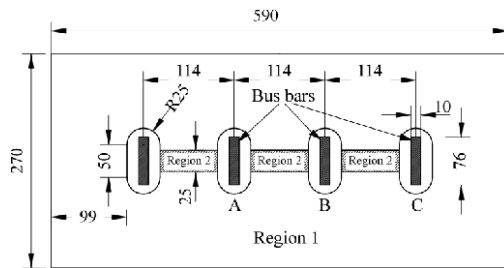


Fig. 1. Geometry of the cover plate with three massive inductors (all dimensions are in mm) [9].

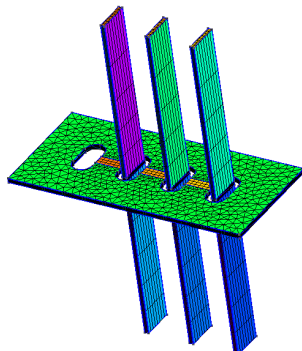


Fig. 2. 3D-dimensional mesh of the cover plate and massive inductors.

$$+ \int_{\Omega} \sigma^{-1} \text{curl} \sum_{n \in N(\Omega_c^c)} \phi_{c,n} v_{c,n} \cdot c_i d\Omega + \int_{\Omega} \sigma^{-1} \text{curl} \sum_{e \in E(\Omega_c)} H_e s_e \cdot c_i d\Omega = -V_i, \quad \forall c_i \in H_h^0(\text{curl}; \Omega). \quad (17)$$

4. Application example

The application is herein a practical test consisting of a cover plate of a transformer of **2000kVA** and three massive inductors (bus bars) shown in Figure 1 [10]. The balanced three – phase currents following in the massive inductors are respectively $I_a = I_{max} \sin(\omega t + 0)$, $I_b = I_{max} \sin(\omega t - \frac{2\pi}{3})$ and $I_c = I_{max} \sin(\omega t + 2\pi/3)$. All dimensions of the cover plate and massive inductors are given in mm, where the cover plate thickness is 6 mm. The cover plate is produced by two different materials (magnetic and non-magnetic regions). The conductivities and relative permeabilities in region 1 and region 2 are respectively $\sigma_1 = 4.07$ MS/m, $\sigma_2 = 1.15$ MS/m, $\mu_{r,1} = 300$ and $\mu_{r,2} = 1$. The problem is tested with $I_{max} = 2.5kA$, and frequency of 50 Hz, 300 Hz and 1000Hz. The scenario of the problem is considered with same and different materials

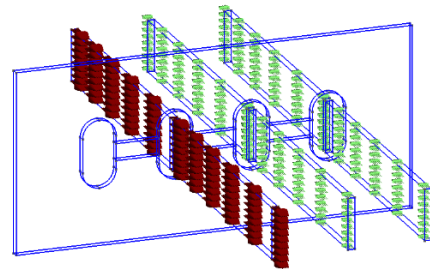


Fig. 3. A three phase current massive inductors.

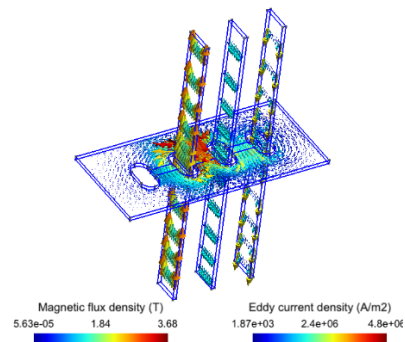


Fig. 4. Eddy current distribution in massive inductors with the same material of the cover plate, for $\sigma_1 = \sigma_2 = 4.07$ MS/m, $\mu_{r,1} = \mu_{r,2} = 300$ and $f = 300$ Hz.

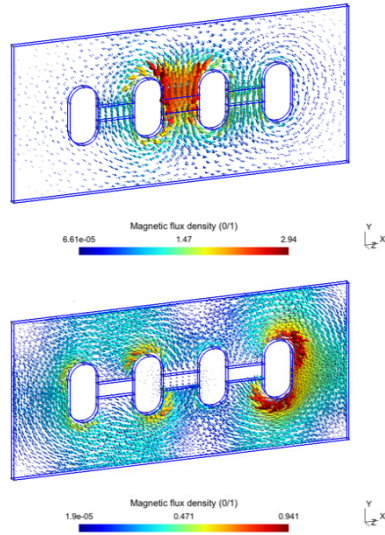


Fig. 5. Magnetic flux density distribution with the same material (*top*) ($\sigma_1 = \sigma_2 = 4.07$ MS/m, $\mu_{r,1} = \mu_{r,2} = 300$) and different materials (*bottom*) ($\sigma_1 = 4.07$ MS/m, $\sigma_2 = 1.15$ MS/m, $\mu_{r,1} = 300$ and $\mu_{r,2} = 1$), for $f = 300$ Hz in both cases.

The first test is solved with the different properties of the cover plate. The 3-D dimensional mesh of the cover plate and three massive inductors is shown in Figure 2, where the cover plate is used triangle meshes and rectangular meshes for three massive inductors. A global three-phase current following in the massive inductors is pointed out in Figure 3. The eddy current distribution in massive inductors due to the global currents (Fig. 3) is pointed out in Figure 4. It can be seen that skin effect maps on the eddy current focus on the surfaces of three massive inductors, for $\sigma_1 = \sigma_2 = 4.07$ MS/m, $\mu_{r,1} = \mu_{r,2} = 300$ and $f = 300$ Hz, skin-depth $\delta = 0.83$ mm. Its skin depth obviously decreases with higher frequencies. Distribution of the magnetic flux density in the cover plate due to the currents in massive inductors is indicated in Figure 5 (*top*). It should be noted that the field value focuses on the surface and in the middle of the cover plate, where the eddy current value is higher than other areas.

The second test is considered with different materials. The field distribution on **B** is presented in Figure 5 (*bottom*). For non-magnetic region of $\mu_{r,1} = 1$, the magnetic field is very small in comparison with the region of $\mu_{r,1} = 300$. It can be shown the areas where the joule power loss is the biggest ($\sigma_1 = 4.07$ MS/m, $\sigma_2 = 1.15$ MS/m, $\mu_{r,1} = 300$ and $\mu_{r,2} = 1$ and for $f = 200$ Hz).

The significant eddy current along the cover plate with effects of different frequencies are depicted in Figure 6. It can be seen that for a higher frequency (e.g.

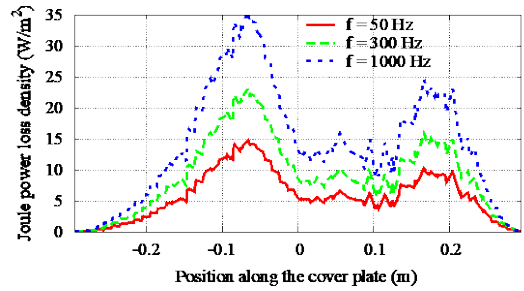


Fig. 6. Eddy current value for same materials along the cover plate with effects of different frequencies ($\sigma_1 = \sigma_2 = 4.07$ MS/m, $\sigma_2 = 1.15$ MS/m, $\mu_{r,1} = 300$ and $\mu_{r,2} = 1$).

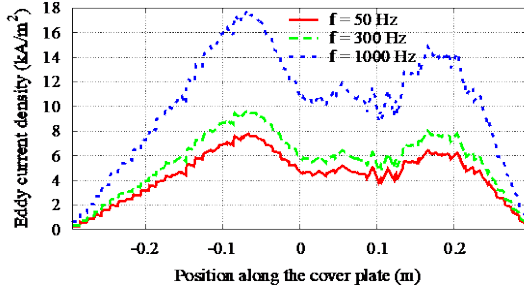


Fig. 7. Joule power loss density for same materials along the cover plate with effects of different frequencies ($\sigma_1 = \sigma_2 = 4.07$ MS/m, $\sigma_2 = 1.15$ MS/m, $\mu_{r,1} = 300$ and $\mu_{r,2} = 1$).

$f = 1000$ Hz), the skin-depth is smaller (i.e. $\delta = 0.45$ mm), the skin effect is greater, the eddy current mainly focus on the surface of the plate, and also with the region of the higher magnetic permeability. In the same way, by integrating of the eddy current along the thickness of the cover plate, the joule power loss density is also expressed in Figure 7 with different frequencies.

5. Conclusion

The numerical method with the **H-Φ** magnetodynamic formulations has been successfully developed for modeling of massive inductors. The presented method permits to evaluate local and global fields (electric current, eddy current loss, magnetic flux, and eddy current loss) taken skin effects into account with different frequencies. In particular, with the obtained results, the method shows the general picture where the field distribution appears. This is also a good step to study thermal problems in electromagnetic devices in next study.

The discretized magnetodynamic formulation has been done for the practical problem in the frequency domain with the linear case. The expanded method can be implemented for non-linear cases.

References

[1] S. Koruglu, P. Sergeant, R.V. Sabarieqo, Vuong. Q. Dang, M. De Wulf, Influence of contact resistance on shielding efficiency of shielding gutters for high-voltage cables, IET Electric Power Applications, Vol.5, No.9, (2011), pp. 715-720.

- [2] G. Meurier, The finite element method for electromagnetic modeling, Wiley, 2008.
- [3] R. V. Sabariego, The Fast Multipole Method for Electromagnetic Field Computation in Numerical and Physical Hybrid System, Ph. D thesis, 2006, University of Liege, Belgium.
- [4] P. Dular, R. V. Sabariego, M. V. Ferreira de Luz, P. Kuo-Peng and L. Krahenbuhl, Perturbation Finite Element Method for Magnetic Circuits, IET Sci. Meas. Technol., Vol. 2, No.6, (2008) 440-446.
- [5] Vuong Dang Quoc and Christophe Geuzaine Using edge elements for modeling of 3-D Magnetodynamic Problem via a Subproblem Method, Sci. Tech. Dev. J.; 23(1) :439-445.
- [6] Patrick Dular, Ruth V. Sabariego, Mauricio V. Ferreira de Luz, Patrick Kuo-Peng and Laurent Krahenbuhl "Perturbation Finite Element Method for Magnetic Model Refinement of – Air Gaps and Leakage Fluxes, Vol 45, No.3 (2009) 1400-1404.
- [7] Vuong Q. Dang, R.V. Sabariego, L. Krähenbühl, C. Geuzaine, Subproblem Approach for Modeling Multiply Connected Thin Regions with an h-Conformal Magnetodynamic Finite Element Formulation, in EPJ AP (Vol. 63, No.1 (2013)).
- [8] Dang Quoc Vuong and Nguyen Duc Quang, Coupling of Local and Global Quantities by A Subproblem Finite Element Method – Application to Thin Region Models, ISSN 1859-2171 – Advances in Science, Technology and Engineering Systems Journal (ASTESJ), Vol 4, no.2, 40-44 (2019).
- [9] S.V. Kulkarni, J.C. Olivares, R. Escarela-Prerez, V. K. Lakhiani and J. Turowski, Evaluation of Eddy Current Losses in the Cover Plates of Distribution Transformers, IEE Proc. Sci. Meas. Technol, Vol. 151, No. 5, September 2004.
- [10] Dang Quoc Vuong, Modeling of Electromagnetic Systems by Coupling of Subproblems – Application to Thin Shell Finite Element Magnetic Models, PhD. Thesis (2013/06/21), University of Liege, Belgium, Faculty of Applied Sciences, June 2013.